05

Magnetism of nanoporus carbon with manganese clusters

© A.M. Danishevskii[1], B.D. Shanina[2], N.V. Sharenkova[1], S.K. Gordeev[3]

[1] Ioffe Institute, St. Petersburg, Russia
[2] Institute for Semiconductor Physics NASU, Kiev, Ukraine
[3] Central Institute of Materials, St. Petersburg, Russia
e-mail: Alex.D@mail.ioffe.ru

Received December 10, 2021
Revised March 7, 2022
Accepted March 23, 2022

Theoretical calculations of the electron density (taking into account the spin) of a model 16-atom carbon cluster with a manganese atom in a micropore showed that it is energetically favorable for manganese atoms to localize inside the pore and form metal nanoclusters in the carbon micropore. The magnetic moment of an ensemble of atoms surrounding a micropore with one manganese atom in it turned out to be quite large. An experimental method was proposed for introducing manganese clusters into bulk samples of nanoporous carbon with different porous structures, and the effect of these adsorbates on the magnetic properties of the samples was studied. In parallel, X-ray diffraction studies of the samples were carried out. It has been shown that Mn clusters near the surface are rather rapidly oxidized in air, as a result of which peaks associated with oxides predominate in the X-ray diffraction patterns. However, small Mn clusters have also been found. Measurements of the dependence of the magnetization of the samples on the applied field at $T = 295\,\mathrm{K}$ showed the presence of nonlinearity and hysteresis characteristic of superparamagnetism or ferromagnetism.

Keywords: micropores, manganese, spin density, magnetization.

DOI: 10.21883/TP.2022.06.54412.313-21

Introduction

Different aspects of adsorption interaction of atoms of the transition metals (TM): Cr, V, Mn, Pd, Fe, Co, Ni adsorbed on graphite or graphene, with carbon atoms have been discussed in a number of theoretical works [1–6]. It has been shown that the interaction of the electronic terms of the metal atoms and the carbon atoms results in the change of the electric and magnetic properties of appearing complexes. It included the investigation of the situation when the magnetism occurs with non-magnetic TM atoms. In the paper [7] this effect has been studied experimentally for natural graphite intercalated by two-dimensional Pd particles. The magnetism occurrence has been explained on the basis of theoretical papers [8,9] results received for free two-dimensional palladium clusters. However, they have not taken into account the interaction of the electron terms of the atoms of palladium and carbon, which takes place at such a close contact.

A convenient way of experimentally observing adsorption interactions is to introduce the TM clusters into the nanoporous carbons (NPC) having a large specific surface. In the field a number of the experimental investigations [10–12] has been performed along with theoretical reasons (for Pd and Ni).

It should be noted that the NPC samples (which are in English abbreviated as CDC) are compatible with tissues of the human body and their magnetic modifications can be purposefully used in medical applications to deliver medicines to a suffering organ.

Introducing the TM clusters (Pd, Ni, Mn) into the NPC pores results in substantial changes of the electric and magnetic properties of the composite samples produced in this ways [10–13]. In particular, in case of the Pd and Mn clusters, the NPCs have exhibited the magnetism of the samples. The initial NPC samples have been produced of powders or polycrystal carbide granules of the metals, which were modified by annealing in chlorine to be quasi-amorphous media. The conditions of creating the NPC−metal complexes as specified in [10–13] excluded the possibility of formation of metal carbides and the main impact was the adsorption interaction of the electrons terms of the atoms of carbon and the metal, whose efficiency was attributable to small sizes of the micropores of the carbon frame ($0.7-2\,\mathrm{nm}$) and their large specific surface ($\sim 1300-1500\,\mathrm{m^2/g}$).

In [13], we have reported the first observation of the superparamagnetic properties in the NPC sample (C(SiC)) prepared of the SiC powder, when introducing the manganese clusters thereinto. The present paper has continued the said studies.

It has theoretically calculated a model periodic cluster of the carbon atoms with a micropore having the Mn atom and demonstrated that this cluster obtained the magnetic properties due to the interaction of the electrons of the atoms of manganese and carbon.

The experiments described by the present paper have used a method of introduction of the Mn clusters into the NPCs, which is somewhat different in comparison with [13],

and initial NPC samples of the two types with various sizes and a structure of micro- and macropores.

The manganese can have several types of the crystal structures, but up to 700°C the bulk metal manganese is in the stable alpha-phase (the volume-centered lattice, the lattice constant is 0.8918 nm). At the room temperature the manganese−paramagnet but with reduction the temperature it transforms into antiferromagnetic phase. The Neel temperature is 95 K.

However, being an atomic impurity in the manganese-alloyed semiconductors A_3B_5 and A_2B_6 (the semi-magnetic semiconductors), the manganese usually contributes to formation of ferromagnetism in these crystal at the low temperatures. However, in this case the manganese atoms are in a diluted state and individually bonded to structures of a specific semiconductor. In a number of their papers, the authors come to the conclusion that in this case the ferromagnetism is caused by formation of a magnetic polaron.

As presumed in [13], the manganese in the NPC pores can form the nanoclusters in the carbon environment and, depending on a shape and size, the metal and carbon contact surface can substantially change, thereby affecting the adsorption interaction of the components.

1. Theory of the possibility of formation of the carbon cluster with the manganese atom in the micropore and the magnetic properties of such a structure

The Mn atom can occupy two fundamentally different positions in the NPC structure: it can build into the surface layer of the carbon atoms surrounding the pore or invade a pore cavity. In the first case, Mn inevitably oxidizes acting as a simple imperfection of the structure, while in the second case manganese can substantially change the electron density and magnetism of the NPC. Solving this task requires answering to how Mn affects the electron structure and the interatomic bonds in the NPC. For this purpose, we have taken ab initio calculations for the model periodic system of the carbon clusters containing 16 carbon atoms surrounding the pore of the 1 nm size. The closed-pore model was built based on a diamond-like crystal structure with a supercell $3 \times 3 \times 3$, which has only surface atoms left. The electron structure and the full energy of the cell were calculated for the case of the empty pore and then for the pore with a single Mn atom introduced into the center thereof.

The electron structure was calculated by the modern computer software package WIEN-2k, which was developed by a team of the authors [14]. The calculations are based on the theory of density functional by Kohn−Hohenberg−Sham (KHS) [15,16].

The full-potential method of linearized associated planar waves (FLAPW) was used to solve the Kohn–Sham equations (KS). The full potential in this method was also calculated in an iteration process taking into account the fact that the electron density and the Coulomb potential must comply with the Poisson's equation. The exchange-correlation potential was calculated by applying the generalized gradient approximation (GGA) with the Perdew, Burke, Ernzerhof parameters [17], where algebraic expressions of the exchange-correlation energy and the potential contain both the electron density and the gradient terms of the electron density.

The preliminary relativistic calculations taking into account the spin polarization of the electron density were performed for non-interacting atoms using the variation principle and the solution of the Dirac equation. The obtained wave functions form the initial electron density. Based on this density, the Poisson equation was used to calculate the new Coulomb potential and the exchange-correlation potential. After substitution of the obtained potentials into the KS equation, we performed a self-consistent process of the iteration calculation V, ρ, E_{tot}.

Let us define the full energy of the interatomic bonds as $E_{\text{bond}} = E_{\text{tot}} - \Sigma_i E_{at,i}$, where E_{tot} — the full energy of the cell containing 16 C atoms and one Mn atom, $\Sigma_i E_{at,i}$ — the sum of the full energies of the free atoms of carbon and manganese. As a result of the calculation with the accuracy to 10^{-4} Ry, we have obtained that in the manganese-free NPC the full bond energy in the cell is equal to

$$E_{\text{bond}}(16\text{C}) = -1211.19\,\text{Ry} + 1209.936\,\text{Ry} = -1.254\,\text{Ry}, \tag{1}$$

as in the case of the single Mn atom in the cell the cell bond energy becomes equal to

$$E_{\text{bond}}(16\text{C} + 1\text{Mn}) = -3528.557\,\text{Ry} + 3526.974\,\text{Ry} = -1.583\,\text{Ry}. \tag{2}$$

When comparing (1) and (2), it follows that manganese enhances the interatomic bond by $-0.329\,\text{Ry} = -4.47\,\text{eV}$. It is obvious this value is equal to the bond energy of the Mn atom with the carbon environment. It means that it is energetically favorable for the manganese atoms to be localized inside the pore.

The calculation taking into account the spin polarization of the electron density results in that the atom magnet moment of the environment of the carbon pore containing 16 carbon atoms and one Mn atom is equal to $33\,\mu_{\text{B}}$, where μ_{B} — the Bohr magneton. At the same time, spatially, the maximum moment is not at the manganese atom, but in some vicinity between it and the carbon atoms. Thus, the carbon cluster with manganese exhibits magnetization as a result of the interaction of the atoms of carbon and manganese within the overlapping of the electron densities.

In order to enable formation of the manganese cluster inside the carbon pore it is necessary that the pore size is at least 2 nm, whereas the length of the Mn−Mn bond is about 0.5 nm. Performing the above-described process of

calculation for the manganese BCC lattice, it is possible to evaluate the Mn−Mn bond energy, which turns out to be higher than the bond energy with the carbon environment $E_{\text{bond}}(\text{Mn–Mn}) = -6.8\,\text{eV}$. Thus, based on the available data, we can say that clusterization of manganese in the carbon pores is energetically favorable.

2. Preparation of samples for experiments

The manganese clusters were introduced by using the NPC bulk samples as plates of the 1 mm thickness prepared based on the carbide powders SiC and B_4C. These powders were used to form plates on a temporary binder and then they were annealed at the temperature of 1000°C in methane. At the same time, due to partial decomposition of methane with release of pyrocarbon (PC) the carbide powder grains were bounded. The sample porosity after the said treatment was determined by the availability of the macropores between the powder grains and it depended on a powder grain size and the amount of the introduced PC. Then, the plates made of the SiC powder with PC were doped with silicon for implementing the reaction of Si with PC and forming the SiC additional component. After that the samples both of SiC, as well as B_4C were chlorinated to remove the atoms of silicon or boron. The SiC samples were chlorinated at the temperature of 1000°C, whereas silicon was removed both from the SiC initial phase and from the newly formed one, thereby obtaining a higher degree of the microporosity of the sample. For the plates made of B_4C with PC the chlorination temperature was 600°C. The properties and parameters of the porosity of the NPC samples produced after all the said processes are given in the table.

The figures 1, 2 fragments of the microporous structure of the said samples C(SiC) and C(B_4C) produced in TEM.

Properties and parameters of porosity of the NPC samples

Parameters	C(SiC)	C(B_4C)
Average size of fragments of the initial carbide powder	2 μm	5 μm
Relative abundance of PC (wt) before chlorination	25%	28%
Total porosity of the samples (relative volume of the pores)	60.7%	74%
Relative volume of micropores measured by adsorption of benzene vapors	47%	44%
Apparent density of the samples	0.82 g/cm^3	0.58 g/cm^3
Micropore sizes measured by the nitrogen adsorption method (slit micropores)	0.7−0.8 nm	1−2 nm

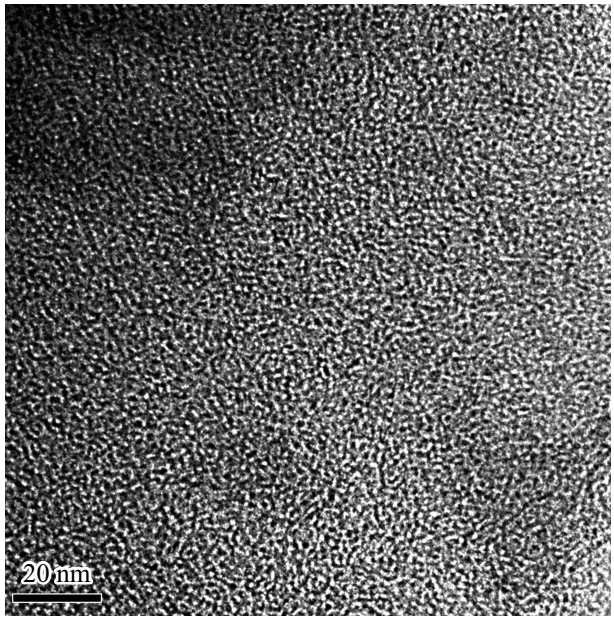

Figure 1. Fragment of the structure of the NPC sample C(SiC) obtained in TEM.

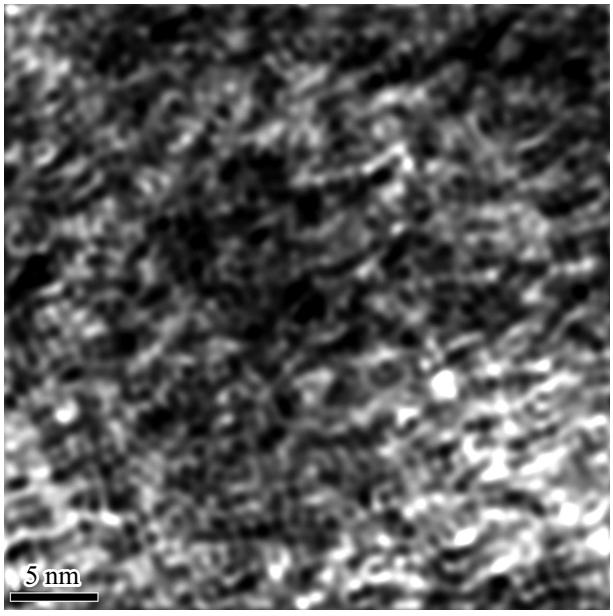

Figure 2. Fragment of the structure of the NPC sample C(B_4C) obtained in TEM.

The plates of the said NPCs and NPCs:Mn were used to prepare the samples for X-ray and magnetometric measurements, too.

In order to introduce Mn into said sample the known reaction of metal recovery from manganese dioxide (MnO_2) at high temperature in reaction with carbon has been used in the present work:

$$MnO_2 + 2C = Mn + 2CO \uparrow . \qquad (3)$$

Of course, first of all, it was necessary to introduce MnO_2 into the NPC pores. The following reaction was used to introduce MnO_2 into the samples:

$$2KMnO_4 + H_2O_2 = 2MnO_2 + 2KOH + 2O_2 \uparrow . \qquad (4)$$

At first, the NPC samples were boiled for longer periods of time in the aqueous solution of potassium permanganate, then taken from this solution and dipped into the 3% hydrogen peroxide solution, which was slowly brought to boiling. At this, there was evidently intense release of gas bubbles, apparently, oxygen, as it must be as per the reaction (4). However, it should be noted that the manganese dioxide resulting from the reaction (4) catalyses the decomposition of the hydrogen peroxide, and in this regard the samples were dipped into the fresh solution H_2O_2 at least three times.

Apparently, quite large molecules of the compounds in the said solutions, first of all, enter the macropores of the NPC samples and only with time and at higher temperatures they penetrate the larger micropores. That is why for the C(SiC) samples having a relatively smaller volume of the macropores and smaller sizes of the micropores, the operations of NPC sample boiling in the solutions $KMnO_4$ and then in H_2O_2 were performed three times. After the said procedures, the samples were dried at the temperature of 60°C and after drying they were annealed in the atmosphere of flowing argon at the temperature of 660°C for 4.5 h in order to realize the chemical reaction (3) therein. At the same time, the MnO_2 molecules formed in the NPC pores react with atoms included in carbon walls of the pores of the NPC samples, thereby increasing the volume of these pores.

On completion of the annealing and cooling of the composite samples to the room temperature, the NPC : Mn plates designed for X-ray measurements were slightly grounded (some dark-gray film was visible on the surface thereof) on a sandpaper with a grain size of 20 μm and immediately placed into tightly closed glass vessels with H-hexane in order to avoid oxidation of the introduced Mn clusters. The X-ray measurements were performed one day later after annealing the samples in the Ar atmosphere. The small samples designed for the magnetometric measurements were weighed (without being grounded) and immediately placed into the tightly closed (permeable) textolite capsules.

3. X-ray studies of the samples

The X-ray diffraction was measured using the diffractometer DRON-3 (CuK_α-radiation) in the standard geometry $\Theta-2\Theta$ „for reflection". Figure 3, *a* shows the diffraction patterns of the initial sample C(SiC) *1* and the similar sample (of the same NPC plate) with introduced manganese *2*. The X-ray radiation for samples with introduced manganese is significantly higher absorbed and dissipated by the sample than for the NPC initial samples. That is why, in order

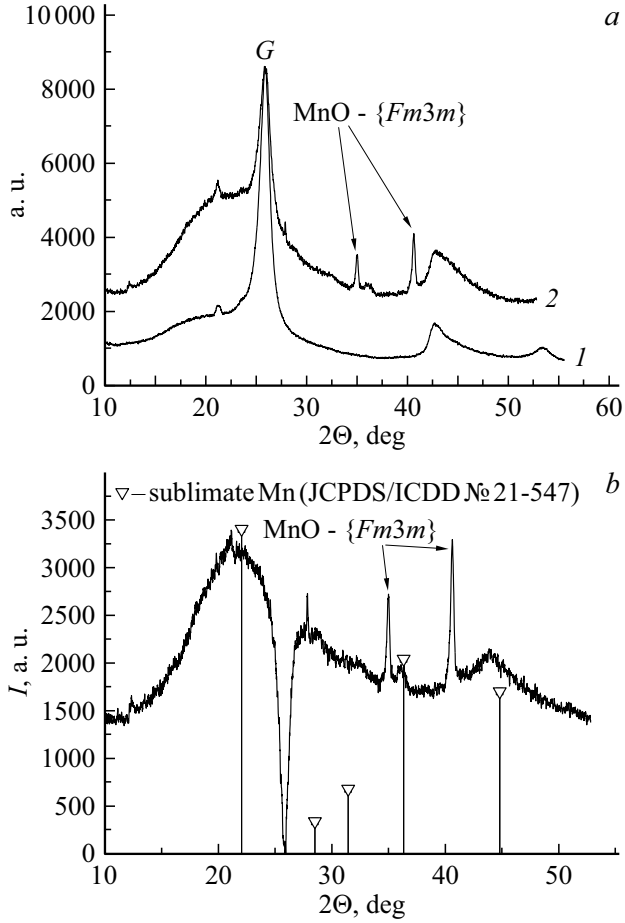

Figure 3. *a* — the diffraction patterns of the samples: *1* — C(SiC); *2* — C(SiC) : Mn (the curve is plotted by the peak amplitudes as a result of equalization of the graphite peak with the similar one in the sample *1*); *b* — the curve of the diffraction pattern difference *2* and *1* (*a*).

to compare peak amplitudes on the said X-ray patterns, it is expedient to built values of these amplitudes as per the amplitude of the peak which should not change when introducing manganese. The intense narrow peak with the maximum at the angle of $2\Theta = 25.86°$ corresponds to a structure of slightly distorted graphite created in the samples C(SiC) due to introduction of a large amount of pyrocarbon at the station of preparation of the NPC initial sample. As the graphite is almost untransformed at the annealing temperature of 660°C required for the Mn oxide recovery reaction (3), the diffraction pattern *2* of Fig. 3, *a* is shown as per peak amplitudes as a result of equating the peak amplitude with the maximum $2\Theta = 25.86°$ to the amplitude of the corresponding peak of the curve *1*. Besides the wide peaks of the NPC carbon structure, the diffraction pattern *2* (Fig. 3, *a*) also includes evident intense narrow peaks corresponding to MnO–Fm3m, but there is no noticeable Mn peak. Although, prior to the measurements the sample had been kept in H-hexane, the sample installation, the beam adjustment and quite long

measurement of X-ray diffraction were in air, and, naturally, the sample surface could be oxidized. The narrowness of the said peaks is indicative of quite large sized of the MnO fragments (for the spherical approximation — ~ 37 nm).

In connection with the above, the curve *1* (Fig. 3, *a*) was subtracted from the reduced curve *2*. Figure 3, *b* shows the difference curve of the diffractograms *2* and *1*, which clearly shows transformations appearing in the composition of the composite sample when introducing the manganese. On Fig. 3, *b*, the designations ∇ also show tabular values of the peak maximums corresponding to one of the possible manganese structures [18]. It can be readily stated that the wide peaks in the vicinity of the angles $2\Theta = 22.1$ and 44.5°, as well as, apparently, 36.2° on the diagram (Fig. 3, *b*) correspond to the manganese nanophase, i.e. to the planes (111), (222) and (202). These manganese fragments, as determined from the peak width $2\Theta = 44.5°$, are sized to be 1.5 nm, so are from the peak width $2\Theta = 36.2°$ — about 13 nm.

The diffraction patterns $C(B_4C)$ — *1* and $C(B_4C):Mn$ — *2* are shown on Fig. 4, *a*. As for the samples C(SiC), the curve for $C(B_4C):Mn$ was also plotted by the point amplitudes as a result of equating the graphite peak amplitude to the graphite peak of the initial NPC ($2\Theta = 26.6°$). The curve *2* has five narrow peaks corresponding to the availability of the MnO cubic phase, but it has not any noticeable features correlated to the availability of manganese. Figure 4, *b* shows the difference curve obtained as a result of subtraction of the X-ray pattern of the initial sample $C(B_4C)$ from the similar curve for the same initial material with manganese introduced thereinto $C(B_4C):Mn$. Besides, Fig. 4, *b* shows literature X-ray data [18], which correspond to one of the manganese modifications. The difference curve of Fig. 4, *b* also has five narrow, very intense MnO peaks, whose availability substantially affects a shape of the whole said curve, thereby complicating identification of features thereof.

However, the said difference curve (Fig. 4, *b*) can be marked with several wide small-amplitude peaks in the vicinity of the angles $2\Theta = 22.1$, 36.3 and 66.2°, which can be attribute to the same structural modification Mn-sublimate [18] as in the samples C(SiC):Mn, with fragment sizes of about 1 nm, which does not exceed the size of the micropores of the initial material $C(B_4C)$.

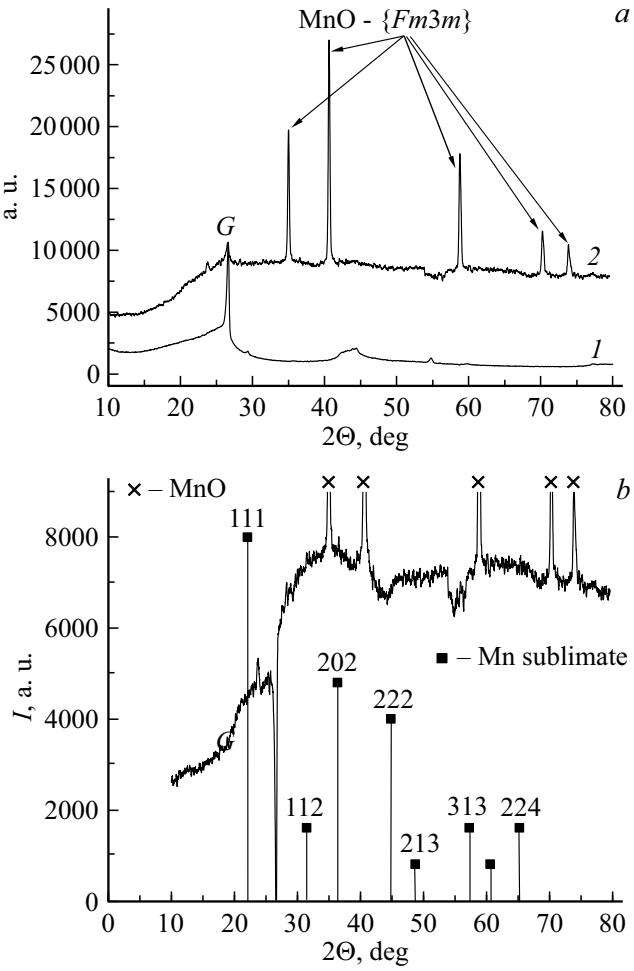

Figure 4. *a* — the diffraction patterns of the samples: *1* — $C(B_4C)$, *2* — $C(B_4C):Mn$ (the curve is plotted by the peak amplitudes as a result of equalization of the graphite peak with the similar one in the sample *1*); *b* — the curve of the diffraction pattern difference *2* and *1* (Fig. 4, *a*).

4. Magnetometric studies

The capsules with the samples for magnetometry were placed into a vibration magnetometer for measurement of the sample magnetization. The said measurements were performed with each sample several times during about one month to reveal the dynamics of the change of its magnetic properties. All this time, the samples were in a closed permeable container and could be gradually oxidized.

This laboratory magnetometer was calibrated by measuring the magnetization curve of the small pieces of the Ni-wire.

Figure 5 shows the dependences of magnetization of the sample on the field for C(SiC):Mn. The curve *1* measured on the next day after sample annealing exhibits the paramagnetic (PM) magnetization nature; the curve *2* measured after the three days already has a kink point indicating its saturation trend in the higher fields. The curve *3* measured 7 days later after annealing has clear magnetization saturation in relatively small fields and small hysteresis, thereby indicating its superparamagnetic (SPM) magnetization nature. But, the measurement performed 28 days later (the curve *4*) again showed the paramagnetic nature of magnetization, thereby indicating oxidation of the main bulk of the metal clusters introduced into the NPC.

The results of measurement of magnetization of the sample $C(B_4C):Mn$ are shown on Fig. 6. For this sample,

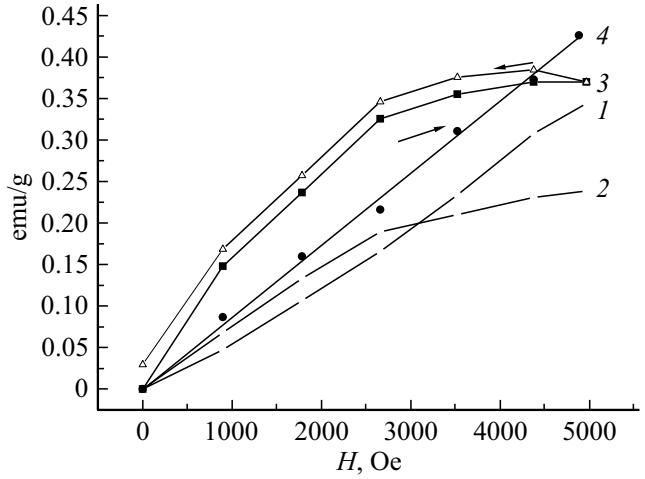

Figure 5. Dependences of magnetization on the field measured for the sample C(SiC) : Mn at the various time intervals: *1* — on the next day after annealing in Ar; *2* — 3 days later after annealing; *3* — 7 days later after annealing; *4* — 28 days later after annealing. $T = 295$ K.

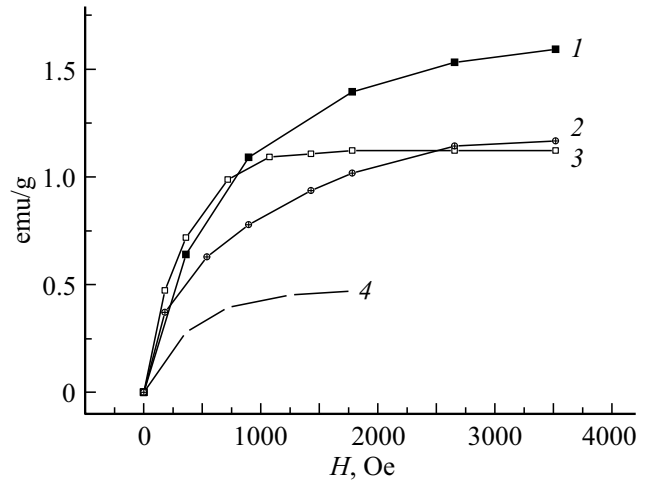

Figure 6. Dependences of magnetization on the field measured for the sample C(B_4C) : Mn at the various time intervals: *1* — on the next day after annealing in Ar; *2* — 2 days later after annealing; *3* — 6 days later after annealing; *4* — 33 days later after annealing. $T = 295$ K.

the magnetizations turned out to be substantially bigger than for C(SiC) : Mn and the magnetization dependence on the field, which is typical for superparamagnetization (SPM) or the ferromagnetic, occurs already at the next day after sample annealing (the curve *1*). With the further measurements (the curves *2*–*4*), the saturation magnetizations are only decreasing. However, even 33 days later after annealing this sample still has the SPM properties. Figure 7 shows the fuller magnetization dependence on the field, which is measured for the sample C(B_4C) : Mn 6 days later after annealing. The measured curves (Fig. 7) were described using a known Langevin formula [19]:

$$I(H) = NM\Big(\mathrm{cth}\big((H \pm H_c)/H_M\big) - H_M/(H \pm H_c)\Big) + (\chi_p - \chi_d)H, \quad (5)$$

where H — the external magnetic field, H_c — the coercive force, χ_p, χ_d — the paramagnetic and diamagnetic susceptibilities of the sample (NPC — the diamagnetics, MnO, MnO_2 — the paramagnetics), $H_M = kT/M$, $M = nS\mu_B$ — the magnetic moment of the superparamagnetic cluster, μ_B — the Bohr magneton, n — the number of spins in the cluster, S — the spin value, N — the concentration of the clusters in the sample. From comparison with the experiment, it is found that $H_c = 150$ Gs, $H_M = 130$ Gs, $M = 3.13 \cdot 10^{-16}$ $(\mathrm{erg} \cdot \mathrm{cm}^3)^{1/2}$, the number of the atoms with the spin $S = 5/2$ in the cluster is $1.4 \cdot 10^4$, while the concentration of these clusters in the sample is $3.8 \cdot 10^{15}$ cl/g. The linear term in the equation (5) turned out to be very small and almost unaffecting the shape of the curves of Fig. 7.

The said magnetic characteristics for C(B_4C) : Mn are naturally related to the fact that the initial NPC sample C(B_4C) had a volume of the macropores which is significantly higher than that of C(SiC), and also had larger micropores. The solutions of the chemical compounds involved in the above-mentioned reaction (4) were more freely entering the macropores and micropores of the NPC C(B_4C) and the number of the appearing clusters MnO_2, as well as their volume turned out to be bigger in comparison with the process of formation of the said clusters in C(SiC). During the reaction (3) proceeded at the temperature of 660°C during 4.5 h, more thin-walled micropores C(B_4C) destroy more easily forming substantially larger pores, which can accept relatively large metal clusters appearing as a result of the reaction (3).

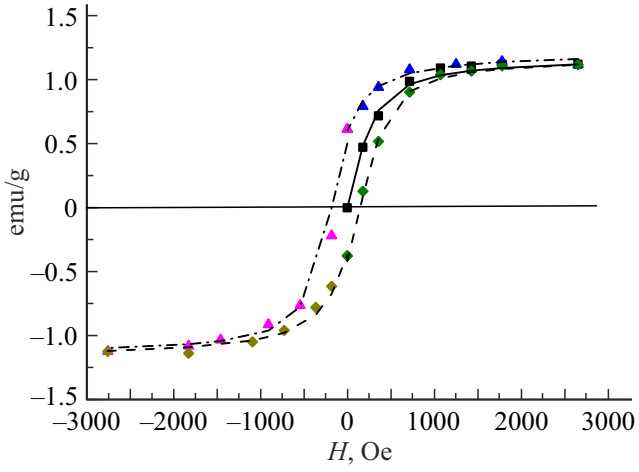

Figure 7. Full magnetization curve measured for the sample C(B_4C) : Mn 6 days later after annealing. $T = 295$ K; the points — the experimental data, the lines — the curves calculated as per the formula (5).

5. Discussion

As the said samples can have manganese oxides MnO, MnO_2 and they as well as manganese itself can have structural and magnetic modifications, it is necessary to discuss their possible impact on occurrence of superparamagnetism of the samples as observed in the experiments. As it is clear from the diagrams of the Figs. 3 and 4, in the studied samples the MnO fragments at the room temperature have the 3*D*-symmetry {Fm3m}. At this phase, they are dielectric paramagnetics with the Neel temperature of 119 K [20], at which they transfer into the antiferromagnetic phase. As the magnetization dependences of the present paper were measured at the temperature of 295 K, the availability of the MnO fraction could affect only the value of the paramagnetic component of the magnetization, but it could not be a cause of formation of the superparamagnetism in the samples. As for MnO_2, then after annealing the samples in Ar this oxide (also the paramagnetic at $T = 295$ K) was not recorded in the X-ray diffraction images. What is the reason of SPM appearance in the sample C(SiC) : Mn only one week later after annealing? We assume that this effect can be correlated to the post-annealing small clusters of manganese and coarsening thereof in time via diffusion due to appearing magnetism by adsorption interaction with the carbon structures surrounding them. It is caused by the electron $s-d$ exchange interaction and the change of the density of the electron states. Thus, with time, very small particles of manganese distributed within the sample bulk are combined by diffusion into larger ones due to indirect magnetic interaction, and those larger ones can include carbon fragments, too, and can exhibit the superparamagnetic properties. For the sample $C(B_4C) : Mn$, the Mn clusters apparently turn out to be quite large to exhibit the SPM properties soon after annealing. However, with time, the metal clusters gradually become oxidized and the sizes of the metallic core of the cluster reduce (apparently, at the same time there is also the decrease in the adsorption interaction of the metal atoms with the carbon atoms) and the occurred SPM magnetization also reduces or obtains the paramagnetic characteristics.

Conclusion

Finally, it can be concluded that the time dependences of the magnetization of the composite samples NPC : Mn typical for SPM are obtained to confirm the availability of the indirect $s-d$ exchange interaction of the Mn atoms via the carbon atoms, which results in the weak magnetism. The said time dependences also allow approximately estimating the existing time of the occurred magnetism, which is limited by metal oxidation in the pores of the carbon sample.

Conflict of interest

The authors declare that they have no conflict of interest.

References

[1] D. Tomanek, W. Zhong. Phys. Rev. B, **43**, 12623 (1991).
[2] S.B. Trickey, F. Muller-Plathe, C.H.F. Dierchsen, J.C. Boettger. Phys. Rev. B, **45**, 4460 (1992).
[3] A. Rakotomahevitra, C. Demangeat, J.C. Parlebas, G. Moraitis, E. Razafindrakoto. J. Phys. Conden. Matter., **4**, 4621 (1992).
[4] A. Rakotomahevitra, G. Garreau, C. Demangeat, J.C. Parlebas. Surf. Sci., **307**–**309**, 1124 (1994).
[5] M. Fudjita, K. Wakabayashi, K. Nakada, K. Kusakabe, J. Phys. Jpn., **65**, 1920 (1996).
[6] H. Sevinçli, M. Topsakal, E. Durgun, S. Ciraci. Phys. Rev. B, **77**, 195434 (2008).
[7] D. Mendoza, F. Morales, R. Escuderes, J. Walter. J. Phys. Cond. Matter., **11**, L317 (1999).
[8] M.J. Zhu, D.M. Bylonder, M. Kleinman. Phys. Rev. B, **42**, 2874 (1990).
[9] S. Boural, C. Demangeat, A. Mokrani, M. Dreysse. Phys. Lett. A, **151**, 103 (1990).
[10] B.D. Shanina, A.M. Danishevskiy, A.I. Veinger, A.A. Sitnikova, R.N. Kyutt, A.V. Shchukarev, S.K. Gordeev. ZhETF, **136** (10), 711 (2009) (in Russian).
[11] A.M. Danishevskiy, T.L. Makarova, A.A. Sitnikova, B.D. Shanina. FTT, **53** (5), 956 (2011) (in Russian).
[12] A.M. Danishevskiy, B.D. Shanina, A.Yu. Rogachev, V.V. Sokolov, A.E. Kalmykov, R.N. Kyutt, S.K. Gordeev. FTT, **59** (10), 2056 (2017) (in Russian).
[13] A.M. Danishevskiy, N.V. Sharenkova, B.D. Shanina, S.K. Gordeev. Pis'ma v ZhTF, **45** (9), 43 (2018) (in Russian).
[14] P. Blaha, K. Schwarz, G.K.H. Madsen, D. Kvasnicka, J. Luitz. *2001 WIEN2k, An Augmented Plane Wave+Local Orbitals Program for Calculating Crystal Properties* (Karlheinz Schwarz, Techn. Universität Wien, Austria), ISBN 3-9501031-1-2.
[15] P. Hohenberg, W. Kohn. Phys. Rev., **136**, B864 (1964).
[16] W. Kohn, L.J. Sham. Phys. Rev. A, **140**, 1133 (1965).
[17] J.P. Perdew, S. Burke, M. Ernzernhoff. Phys. Rev. Lett., **77**, 3865 (1996).
[18] *Powder diffraction file / Inorganic Phases, Alphabetical index,* JCPDS (ICDD), (USA, 1989), p. 361.
[19] S.V. Vonsovskiy. *Magnetism* (Nauka, M., 1971), p. 807 (in Russian).
[20] A.M. Balagurov, I.A. Bobrikov, S.V. Sumnikov, V.Yu. Yushankhai, N. Mironova-Ulmane. Pis'ma v ZhETF, **104** (2), 84 (2016) (in Russian).